The Yucatan minipig model: A new preclinical model of malnutrition induced by a low-calorie/low-protein diet

Laurence Lacaze, Sarah Rochdi, Annaëlle Couvert, Steve Touboulic, Sylvie Guerin, Gwenaelle Randuineau, David Martin, Véronique Romé, Charles-Henri Malbert, Frédéric Derbré, et al.

The Yucatan minipig model: A new preclinical model of malnutrition induced by a low-calorie/low-protein diet

Laurence Lacaze[1,2], Sarah Rochdi[2], Annaëlle Couvert[3], Steve Touboulic[2], Sylvie Guérin[2], Gwénaëlle Randuineau[2], David Martin[3], Véronique Romé[2], Charles-Henri Malbert[4], Frédéric Derbré[3,*], David Val-Laillet[2,*], Ronan Thibault[1,2,*]

* *These authors contributed equally as last author*

[1] Unité de Nutrition, service Endocrinologie-Diabétologie-Nutrition, CHU Rennes, Rennes, France

[2] INRAE, INSERM, Univ Rennes, NuMeCan, Nutrition Metabolisms Cancer, Rennes, France

[3] Laboratory "Movement Sport and Health Sciences" EA7470, University of Rennes/ENS Rennes, France

[4] INRAE, PRISM Ani-Scans, St Gilles, Rennes, France

Corresponding authors:

Prof. Ronan THIBAULT

Centre labellisé de nutrition parentérale au domicile - CHU Rennes

2, rue Henri Le Guilloux, 35000 Rennes, France

Tél. +33 2 99 28 96 46 / Fax +33 2 99 28 24 34

E-mail ronan.thibault@chu-rennes.fr

Dr Frédéric DERBRÉ

Laboratory "Movement, Sport and Health Sciences" EA 7470

University of Rennes, ENS Rennes, 35170 Bruz, France

Email: frederic.derbre@univ-rennes2.fr

ABSTRACT

Background & Aims. Severe malnutrition exposes patients to adverse outcomes and a higher mortality risk. The Yucatan minipig, closer to human physiology than murine models could be a pertinent and innovative experimental model for studying the physiopathology and consequences of severe malnutrition. The present study aimed to determine whether a low calorie/low protein diet (LC/LP) can reproduce marasmus malnutrition in minipigs, and to characterize body composition, gut microbiota, malnutrition-related blood parameters, and histological and molecular skeletal muscle patterns.

Methods. Eleven Yucatan minipigs were subjected to two different diets: a standard control diet (ST) (n=5) and a LC/LP diet (n=6). LC/LP animals daily received 50% of an isocaloric low-protein diet (10.37 MJ/kg, 8.6% protein). Body composition was measured by computed tomography (CT-scan) before (T0) and after 8 weeks of diet (T8). *Trapezius* and *biceps femoris* muscles were sampled at the end of protocol to perform histological and molecular analyses. Gut microbiota composition ~~were~~ was also analyzed at T0 and T8 in fecal samples.

Results. Eight weeks of LC/LP diet significantly reduced body weight (-12.3±9.5%, P=0.03) and gut microbiota richness (*i.e.* number of observed species) (-10.4±8.3%, P=0.014) compared to baseline. After 8 weeks, LC/LP animals exhibited a significant reduction of retroperitoneal fat and skeletal muscle surface areas (P=0.03 and P=0.047, respectively), whereas these parameters remained unchanged in ST animals. These reductions were associated with lower muscle fiber cross-sectional area (CSA) in *trapezius* (P<0.001) and *biceps femoris* (P=0.003) in LC/LP animals compared to ST. LC/LP diet promoted an increase of AMP kinase phosphorylation in *trapezius* and *biceps femoris* (P=0.05), but did not affect cytochrome c and COX IV protein content, markers of mitochondrial content. Gene and proteins involved in ubiquitin-proteasome system and apoptosis remained unchanged after 8 weeks of LC/LP diet both in *trapezius* and *biceps femoris.*

Conclusion. All these findings support that this experimental minipig model of severe malnutrition is valid to mimic pathophysiological changes occurring in human protein-energy marasmus malnutrition and muscle atrophy associated with malnutrition, as observed in patients with secondary sarcopenia .

KEYWORDS: undernutrition, muscle atrophy, energy metabolism, sarcopenia, protein synthesis

NO-STANDARD ABBREVIATIONS:

4EBP1: eukaryotic translation initiation factor 4E binding protein 1; Akt: protein kinase B; ALT: alanine transaminase; AMPK: adenosine monophosphate-activated protein kinase; AST : aspartate transaminase; Bax: Bcl-2–associated X protein; Bcl-2: B-cell lymphoma 2; CRP: c-reactive protein; CT-scan: computed tomography; COXIV: cytochrome c oxidase subunit IV; FSR: fractional synthesis rate; GLUT4: glucose transporter type 4; IP3K: inositol 1,4,5-trisphosphate 3-kinase; MAFbx: muscle atrophy F-box; mTORC1: mammalian target of rapamycin 1; MuRF1: muscle ring finger-1; p70S6K: Ribosomal protein S6 kinase beta-1

INTRODUCTION

The medical costs due to diseases associated with malnutrition are evaluated at more than 31 billion dollars in Europe and 9.5 billion dollars in the United States of America [1,2]. Among the different forms of malnutrition, the protein-energy malnutrition is observed in several clinical situations including anorexia nervosa, cancers, cirrhosis, inflammatory bowel disease, chronic renal failure, but also in some forms of obesity [3,4]. Malnourished patients frequently exhibit sarcopenia, defined as a loss of muscle mass and strength and physical performance, exposing them to adverse outcomes and a higher mortality risk [5,6].

The cellular mechanisms involved in the loss of muscle mass have been extensively explored in sarcopenia related to aging, cancer or immobilization [7–9]. The loss of muscle mass results from an imbalance of myofibrillar protein turnover due to an exacerbation of proteolysis and/or a reduction of protein synthesis in muscle fibers. On one hand, proteolysis can be exacerbated by an activation of calpains, cathepsins, caspases, ubiquitin-proteasome and autophagy-lysosome systems, which act synergistically to stimulate protein breakdown [7,10]. On the other hand, an alteration in the activity of the PI3K/Akt/mTORC1 signaling pathway is identified as playing a key role in the reduction of protein fractional synthesis rate (FSR) in atrophied skeletal muscle [11–13]. Muscle apoptosis is also likely to play an important role in the reduction of protein synthesis in atrophied skeletal muscles, even if a debate still exists about the muscle cell population where it occurs (*i.e.* myofibers, satellite cell, endothelial cells) [14,15]. In malnourished patients, these cellular mechanisms could be ~~activated~~ affected both by a protein-energy deficit (*e.g.* anorexia nervosa) or/and to the hypermetabolism related to diseases (*e.g.* liver cirrhosis, cancer, inflammatory bowel disease, critical illness). Interestingly, gut microbiota dysbiosis is reported in anorexia nervosa patients with marasmus malnutrition [16], but also in mice and patients exposed to low-protein diet [17,18]. Such dysbiosis has been recently proposed as playing a potential role in sarcopenia development [19].

During the last decade, several experimental models have been developed, essentially in rodents, to better understand the cellular mechanisms involved in sarcopenia related to malnutrition. Some of these rodent models reproduce the hypermetabolism related to chronic diseases [20,21], others induce a drastic protein-energy restriction to mimic marasmus or kwashiorkor [22,23]. Though, the rodent models present several limitations related to their phylogenetic distance and significant differences compared to humans in terms of eating behavior, circadian rhythm and general anatomy. These discrepancies can make the transposition and analogy to humans difficult when studying the pathophysiological mechanisms of malnutrition. The minipig has recently emerged as an alternative and innovative experimental model to explore physiological mechanisms related to malnutrition, including amino acids metabolism or eating behavior [24,25]. Except for the non-human primates, the pig presents the advantage to be the experimental model the closest from human physiology among all the animal models used in nutrition research [26]. ~~Finally, minipigs are smaller than the standard pigs and offer the possibility to explore at the adult age the body composition with the same devices as in humans, such as the computed tomography-scan (CT-scan) [27]~~.

Therefore, the purpose of the present study was to develop with the minipig a preclinical animal model of malnutrition close to human marasmus, as especially observed in anorexia nervosa. To validate this experimental model, we determined in Yucatan minipigs the effects of a low-calorie/low-protein (LC/LP) diet on body composition, gut microbiota, malnutrition-related blood parameters, and histological and molecular skeletal muscle patterns.

MATERIALS AND METHODS

Animal experiments were approved by The Regional Ethics Committee in Animal Experiment of Brittany (APAFIS # 16413-2018080711214660 v2) and validated by the French Ministry of Research in accordance with the current ethical standards of the European Community

(Directive 2010/63/EU as amended by Regulation (EU) 2019/1010). All experiments were performed at the INRAE UE3P experimental facilities for pig physiology and phenotyping, under Agreement No. C35-275-32 and individual Authorization No. 35-88 (DVL).

Animals and diet. Eleven 30-month-old Yucatan minipigs were randomly distributed into two experimental groups: A standard diet group (ST, n=5, 4 females and 1 male) and a low-calorie/low-protein diet (LC/LP, n=6, 5 females and 1 male). The two different diets were isocaloric: a standard diet (10.33 MJ/Kg, 15% protein) and a low-protein diet (10.37 MJ/kg, 8.6% protein). The composition of the two types of food is detailed in **Table 1**. The ST diet was similar to that given to all animals in the months and years preceding this experimentation. ST ration was calculated on the basis of the metabolic weight ($MW=LW^{0.75}$, where LW is the live weight in kg) of the animals, energy requirements and the energy composition of the food. The normal energetic ration for a normal-weight adult Yucatan minipig is 0.3017 MJ/kg MW. LC/LP diet consisted in half of this daily ration, *i.e.* 0.1508 MJ/kg. The food ration for each animal was calculated and corrected on individual weight every two weeks. All animals were housed in individual pens (120 cm x 85 cm) with standard conditions for temperature (22-23°C), light/dark cycle (12h/12h) and a free access to tap water. The animals were weighed at the beginning, and then every two weeks until the end of the experiment. After 8 weeks of diet, minipigs were sacrificed with electronarcosis followed by immediate exsanguination in the morning in fasting condition. Skeletal muscles (*i.e. Biceps Femoris*, *Trapezius*) were sampled immediately after euthanasia, weighed and frozen in liquid nitrogen or fixed in 4% paraformaldehyde (PFA). Blood was centrifuged (1500 *g* for 10 min) for plasma collection. Stool samples were collected before (T0) and at the end of the protocol (T8).

Computed tomography-scan (CT-scan) body composition measurement. CT-scan were performed under general anesthesia at the beginning of the experiment (T0) and after 8 weeks of diet (T8) as previously described [27]. Briefly, cross-sectional scans were acquired at the

thoracic vertebra T13 to determine adipose tissue and muscle (*i.e. Longissimus dorsi, Psoas major and large muscle*) areas. Despite intra-abdominal fat could be separated into two compartments [27], visceral fat (*i.e.* inside the peritoneum) and retroperitoneal fat, in our study, only the retroperitoneal fat was considered because of major feces artefacts and the thinness of some pigs, which complicated the assessment of visceral fat and represented a potential bias for the analyses. Muscle and fat areas were measured using ImageJ software (National Institutes of Health, Rockville, MD, USA). As in humans, a muscle density range for CT-scan was considered between -29 and +150 Hounsfield units (HU) and a fat density range was considered between -190 and -30 HU.

Plasma analyses. C-Reactive Protein (CRP) levels were determined using ELISA kit purchased from Immunology Consultant Laboratory (Portland, USA). Alanine aminotransferase (ALT), aspartate aminotransferase (AST), urea, creatinine, glucose, and albumin were measured using a Konelab automated system and specific detections kits for each parameter purchased from Thermo Fisher Scientific (Illkirch, France).

DNA extraction from feces and sequencing. Total cellular DNA was extracted from animal fecal material using the ZR Fecal DNA MiniPrepTM kit (ZymoResearch, USA). DNA concentration was then determined at 260 nm using a nanospectrophotometer (Denovix, Wilmington, USA). The V3-V4 region of the 16S rRNA gene was then amplified by using the primers F343 (5'-CTTTCCCTACACGACGCTCTTCCGATCTACGGRAGGCAGCAG-3') and R784 (5'-GGAGTTCAGACGTGTGCTCTTCCGATCTTACCAGGGTATCTAATCCT-3') modified to add adaptors during the second PCR amplification [28]. Sequencing was performed using the MiSeq technology (Illumina) at the Genopole Toulouse Midi-Pyrenees (GeT) genomics facility (https://get.genotoul.fr/).

Metagenomics analysis. The 16s ribosomal RNA raw sequences were analyzed using the bioinformatic pipeline FROGS (Find Rapidly OTU with Galaxy Solution)[29]. Briefly, this

pipeline includes a preprocessing step where reads are merged with FLASH [30], dereplicated, and filtered according to their length, mismatches in primers with cutadapt [31] and N content. This step is followed by Swarm clustering [32] with an agglomeration distance of d=3. Chimera detection is then performed using Vsearch [33] before applying an OTU abundance filter (OTUs < 0.005% of the total abundance are discarded) [34]. The most abundant sequences of each OTUs were then affiliated with BLASTn against the Silva v132 database [35]. Estimates of bacterial OTU diversity were estimated using the Shannon and Simpson indexes, in addition to observed richness and Chao1 indexes. β-diversity analyses were performed on Bray-Curtis distances matrix of DNA samples and were then visualized using principal coordinate analysis and the ggplot2 R package.

Histological analyses. *Biceps femoris* and *trapezius* muscle samples were fixed in formalin, embedded in paraffin and then cut into serial 10-µm-thick slices using a LEICA microtome. These slices were then stained with hematoxylin-eosin. In *trapezius* muscle samples only, complementary slices were also stained with monoclonal antibodies targeting type 2 fast and type 1 slow myosin isoforms as previously described [36]. Image acquisitions were performed at x10 magnification using a microscope (Nikon Eclipse 80i) and analyzed using ImageJ software [37]. Six muscle fields per animal were analyzed, and all muscle fibers in each group were pooled for statistical analysis (500-900 fibers/group).

RNA extraction and quantitative real time PCR. Total RNA from *trapezius* and *biceps femoris* were extracted using Qiagen RNeasy Plus Universal Mini Kit according to the manufacturer's protocol. RNA amounts were determined by Denovix spectrophotometer, and RNA quality was controlled using the Agilent 2100 Bioanalyzer (Agilent Technologies, Palo Alto, CA). Reverse transcription reaction (RT) was carried out on 1 µg of total RNA (IScript reverse transcription, 170-8840). Then, real-time PCR experiments were performed on RT products in a final volume of 12.5 µl containing: 2.5 µl of cDNA (diluted at 1/40), 0.75 µl of

primers (5 µM) and 6.25 µl of SYBR® Green Supermix (1725271, Biorad) and 3 µl of ultrapure water. Experiments were monitored in CFX Real-Time machine (Biorad). The expression of target genes was normalized to reference genes and the relative expression was calculated using the ΔΔCt method. Primer sequences are listed in **Supplemental Table 1**. The reference genes were TATAbox Binding Protein1 (*Tbp1*), ribosomal protein L4 (*Rpl4*) and hypoxanthine phosphoribosyltransferase1 (*Hprt1*).

Cytosolic protein extraction. Skeletal muscles were grounded in liquid nitrogen and the obtained powder was used to perform extraction. Cytosolic protein extraction was performed from *trapezius* and *biceps femoris* in cold lysis buffer containing 10.0 mM Tris·HCl, pH 7.4, 0.5 M sucrose, 50.0 mM NaCl,5.0 mM EDTA, 30.0 mM Na4P2O7, 1% NPosP-40, 0.25% sodium deoxycholate, 50.0 mM NaF, 100.0M sodium orthovanadate, and protease inhibitor cocktail (5l/ml, P8340; Sigma, St. Louis, MO). The samples were homogenized using a Polytron homogenizer at 4°C. Each sample was then incubated on ice for 30 min followed by 10 s of sonication. The homogenates were then transferred to microcentrifugation tubes and centrifuged at 12,000g for 12 min at 4°C. The protein concentration of the supernatant was determined by a Lowry assay using bovine serum albumin as a standard.

Western blotting. Samples were diluted in SDS-PAGE sample buffer (50 mM Tris·HCl, pH 6.8, 2% SDS, 10% glycerol, 5%-mercaptoethanol, and 0.1% bromophenol blue) and heated 5 min at 95°C until analyses. Samples containing 50 µg of proteins were resolved on 10% or 12.5% SDS-PAGE. The proteins were transferred at 240 mA for 90 min onto a 0.2-µm nitrocellulose membrane. Membranes were blocked with 5% BSA or non-fat dry milk in Tris-buffered saline/0.05% Tween-20 (TBST) for 1h at room temperature. Membranes were incubated overnight at 4°C with appropriate primary antibodies (**Supplemental Table 2**). Thereafter, membranes were washed with TBST and incubated for 1h at room temperature with infrared dye-conjugated secondary antibodies (LI-COR, Lincoln, NE). After being washed,

blots were captured using the Odyssey Imaging System (LI-COR). All blots were scanned, and densitometry analysis of the bands was conducted using GS-800 imaging densitometer and Quantity One software (Bio-Rad Laboratories, Inc.). All blots were corrected for loading based on the HSC70 expression.

Statistical analyses. All data are presented as the mean ± standard deviation (SD). Mann-Whitney tests were performed to explore the effects of LC/LP diet compared to standard diet on histological and biological parameters. Wilcoxon signed-rank tests were performed to explore the same effects on body weight, CT-scan data and gut microbiota indexes. To assess β-diversity of gut microbiota, distance matrices between samples were generated on the basis of Bray-Curtis dissimilarity and reported in Multi-dimensional Scaling (MDS). For all statistical analyses, the significance level was set at 0.05. Statistical trends were considered for 0.05<*P*-value<0.10. Data were analyzed using the statistical package GraphPad Prism version 8.00 for Windows (GraphPad Software, La Jolla, California).

RESULTS

Effects of LC/LP diet on body weight and body composition. Body weight and body composition variations before and after 8 weeks of standard or LC/LP diet are shown in **Figure 1**. While the ST diet had no effect on body weight (**Fig. 1A**), we reported a significant weight loss after 8 weeks of LC/LP diet (-12.3±9.5%, p=0.03, **Fig. 1A**). We observed a significant decrease in T13 muscle area determined by CT-scan after 8 weeks of LC/LP diet (from 11866±1657 mm² to 11142±1057 mm², *P*=0.046, **Fig. 1B**), whereas this parameter remained unchanged in the ST group (**Fig. 1B**). Similarly, a significant reduction in retroperitoneal fat area occurred after 8 weeks of LC/LP diet (from 10626±4380 mm² to

8073±3808 mm², *P*=0.015, **Fig. 1C**), while this parameter remained unaffected in the ST group (**Fig. 1C**).

Effects of LC/LP diet on muscle fiber size. Muscle fiber cross-sectional area (CSA) histological analyses have been performed both in *biceps femoris* and *trapezius* muscles. These results are shown in **Figure 2**. Muscle fiber CSA were significantly lower in the LC/LP group compared to the ST group both in the *trapezius* (-34%, *P*<0.001, Fig. **2A-C**) and in the *biceps femoris* muscles (-15%, *P*<0.001, **Fig. 2D-F**). Type 1 slow fiber CSA were significantly lower in the LC/LP group compared to the ST group in the *trapezius* (-28.9%, *P*<0.001, **Fig. 2G and 2H)**. Similarly, type 2 fast fiber CSA were significantly lower in the LC/LP group compared to the ST group in the *trapezius* (-38.4%, *P*<0.001, **Fig. 2G and 2I)**.

Effects of LC/LP diet on plasma biochemical parameters. Plasma biochemical parameters measured in blood samples obtained after 8 weeks of diet are presented in **Table 2**. Urea plasma level significantly decreased in the LC/LP compared to the ST group (from 371±88 to 236±40 mg/l, *P*=0.008), while the plasma creatinine level significantly increased from 15.5±0.9 to 17.9±1.4 mg/l, *P* =0.017). Plasma albumin and glucose levels did not differ between LC/LP and ST groups. AST levels were significantly lower in the LC/LP group compared to the ST group (from 79.3±19.7 to 41.0±11.9 mg/l, *P*=0.016), whereas LC/LP diet decreased plasma ALT levels (from 55.2±13.0 to 39.0±7.3 mg/l, *P*=0.05). Plasma CRP levels remained unchanged in LC/LP compared to ST groups.

Effects of LC/LP diet on gut microbiota composition. Data related to the impact of the ST and LC/LP diets on gut microbiota composition are shown in **Figure 3**. While the ST diet had no effect on gut microbiota richness (*i.e.* number of observed species and Chao1) and α-diversity indexes *(i.e.* Shannon and Simpson) (**Fig. 3A)**, we reported a significant reduction of the number of observed species after 8 weeks of LC/LP diet (-10.4±8.3%, p=0.014, **Fig. 3B**). Similarly, the Chao1 index tended to decrease after 8 weeks of LC/LP diet (-9.6%±9.9%,

p=0.07, **Fig. 3B**). PERMANOVA tests show that 8 weeks of LC/LP diet slightly influenced the β-diversity based on Bray–Curtis dissimilarity index (r^2=0.23, p=0.005, **Fig. 3E**), whereas no significant difference was reported after 8 weeks of ST diet (**Fig. 3D**). The abundance of the main phyla of gut microbiota remained unaffected after 8 weeks of standard or LC/LP diet (**Fig 3C**). A significant correlation was observed between the variations of the number of observed species and the body weight between T0 and T8 (r=0.68, p=0.02, **Fig. 3F**).

Effects of LC/LP diet on signaling pathways involved in energy metabolism and muscle atrophy. LC/LP diet significantly increased the phosphorylation of AMP kinase (AMPK) both in *trapezius* and *biceps femoris* (p=0.051, **Fig. 4B and D**). COXIV and cytochrome c protein levels remained unchanged after 8 weeks of LC/LP diet both in *trapezius* and *biceps femoris* (**Fig. 4B and D**). After 8 weeks of diet, protein ubiquitination, as well as MuRF1 and MAFbx mRNA and protein levels, did not differ between ST and LC/LP groups in *trapezius* and *biceps femoris* (**Fig. 4B and D, Fig. 5A-B**). Whereas phosphorylation of 4EBP1 and P70S6K protein content remained unaffected after 8 weeks of LC/LP diet, we observed a significant increase of Akt phosphorylation levels both in *trapezius* and *biceps femoris* (*P*=0.05 and *P*=0.0087, respectively, **Fig. 4B and D**). Protein expression of *Bax* and Bcl-2 *apoptotic* factors did not differ between ST and LC/LP groups whatever the skeletal muscle explored (**Fig. 4B and D**). The mRNA levels of myostatin tended to decrease in *trapezius* muscle (**Fig. 5A**), whereas no significant changes were reported in *biceps femoris* (**Fig. 5B**).

DISCUSSION

The objective of the present study was to develop an experimental and innovative preclinical model of protein-energy malnutrition (*i.e.* marasmus) in the Yucatan minipig, to characterize the histological and molecular skeletal muscle patterns of these animals, and to approach the underlying mechanisms. We observed that the LC/LP diet decreased body weight, abdominal

fat mass and muscle mass determined by CT-scan and gut microbiota richness, supporting the validity of our model to mimic the clinical picture of a protein-energy malnutrition. The concomitant reduction of muscle fiber CSA reported in both *biceps femoris* and *trapezius*, combined with CT-scan data, also support that this malnutrition experimental model could promote ~~sarcopenia~~ muscle atrophy. All together, these data highlight that our LC/LP diet in minipigs is a valid experimental model to explore human marasmus malnutrition.

The recent Global Leadership Initiative on Malnutrition (GLIM) consensus report defined that a severe malnutrition occurs when a patient exhibits a body weight loss higher than 10% in the past 6 months [38]. In the present study, we observed a weight loss higher than 10% in minipigs after 8 weeks of LC/LP diet, which supports a severe malnutrition state. The longitudinal exploration of body composition by CT-scan also showed reductions in both abdominal fat and muscle surfaces in LC/LP animals, which ~~confirms this state of severe malnutrition~~ is in accordance with the data reported in human marasmus (i.e. anorexia nervosa patients) [39,40]. In parallel, we measured the muscle fiber CSA in *biceps femoris* and *trapezius*, two skeletal muscles with distinct contractile phenotypes. The *trapezius* possesses indeed a majority of slow twitch fibers, whereas *biceps femoris* expresses a majority of fast twitch fibers [41]. Here, we report that LC/LP animals exhibited smaller muscle fiber CSA in both *biceps femoris* and *trapezius*, which is in agreement with our CT-scan data and with histological data obtained in marasmic patients [40,42]. In *trapezius* muscle, we specifically observed that both type 1 and type 2 CSA significantly decreased in LC/LP animals compared to ST animals, and that the decrease tended to be greater for type 2 fibers. These results are in agreement with data collected in anorexia nervosa patients supporting higher atrophy in fast than slow fibers [40,42–44]. Altogether, these results support the validity of our experimental model to mimic structural muscle adaptations occurring in protein-energy malnutrition reported in human marasmus.

We measured in the plasma of our minipigs the blood biomarkers commonly used for diagnosing malnutrition at hospital in humans. We first observed that LC/LP animals displayed low plasma urea levels, similarly to previous studies performed in rodent or pigs exposed to low-protein diet [17,45]. Protein restriction is indeed well known to affect urea-cycle enzymes, and our results are in accordance with low levels of plasma urea reported in children or adult patients suffering from kwashiorkor [46,47] or protein-energy malnutrition [48,49]. ~~but also with kinetics of plasma urea levels determined in rodent or pig models of low-protein diet.~~ Loss of muscle mass is generally associated with decrease in plasma creatinine levels in malnourished children and adults [50], bedridden patients [51] or sarcopenic older adults [52]. We observed increased plasma creatinine levels in samples from animals exposed to 8 weeks of LC/LP diet. Such an increase could be explained by a renal dysfunction concomitant to muscle mass loss. Indeed, renal dysfunction is generally reported in different forms of protein-energy malnutrition [53,54]. We also observed that plasma albumin levels remained unchanged in LC/LP minipigs, similarly to previous studies in malnourished animals with a low-protein diet [17,55,56], and in accordance with the usually observed normal plasma albumin levels in humans with marasmus malnutrition [38]. All these data associated with the lack of change in plasma CRP levels support the assumption that our experimental model is a severe malnutrition model close to marasmus, with no systemic inflammation.

During the last decade, few studies have investigated the impact of severe malnutrition on gut microbiota composition and function [16,18,57,58]. By performing fecal transplantation from malnourished Malawian children in germ-free mice, a marked weight loss and impaired growth compared to control germ-free mice that received microbiota from healthy children were reported [18,57], thus supporting a potential link between gut microbiota composition and malnutrition genesis. Several studies also showed that anorexia nervosa patients exhibit a marked decrease in gut microbiota richness (i.e. observed species and Chao1 index), whereas

the Shannon index, an α-diversity index, remained unchanged compared to healthy controls [16,59]. In the present study, we similarly reported a reduction of gut microbiota richness in LC/LP animals, whereas the α-diversity indexes remained unchanged. Interestingly, we also observed that this reduction of gut microbiota richness was well correlated with body weight loss. All together, these results reinforce the validity of our minipig model of human marasmus malnutrition. Further studies are needed to better understand the pathophysiological role of gut microbiota in malnutrition and sarcopenia.

~~Underlying mechanisms of sarcopenia under LC/LP diet~~. Impact of LC/LP diet on signaling pathways involved in muscle atrophy. Few scientific data are currently available concerning the cellular mechanisms involved in sarcopenia related to protein-energy malnutrition. Deficit in cellular energy is associated with an activation of the energy sensor AMPK. In the present study, we first observed an activation of AMPK both in *biceps femoris* and *trapezius*. These results demonstrate that skeletal muscle is sensitive to the protein-energy deficit induced by our experimental model, which is coherent with a recent study reporting also an activation of this energy sensor in malnourished rats [23]. In physiological situations like physical exercise, the transient energy deficit and concomitant activation of AMPK promotes muscle adaptations to stimulate mitochondrial activity and oxidative metabolism [60]. Under protein-energy malnutrition and chronic energy deficit in skeletal muscle, we observed that both cytochrome c and COX IV protein contents, markers of mitochondrial density, remained unchanged in *biceps femoris* and *trapezius*. The fact that the energy deficit was chronic, and not ~~followed by~~ associated to substantial nutrient intake by skeletal muscles, probably contributes to explain this inability of skeletal muscles to promote mitochondrial biogenesis under severe malnutrition.

The muscle atrophy we observed in minipigs after 8 weeks of LC/CP diet can be explained both by reduced protein synthesis and/or increased proteolysis. Protein synthesis is mainly regulated

by the Akt/mTORC1 signaling pathway that promotes translation initiation and ribosomal protein synthesis through the activation of 4EBP1 and p70S6K, respectively [61]. In the present study, we did not report any changes in activation of 4EBP1 and p70S6K both in *biceps femoris* and *trapezius*. However, protein FSR is known to be reduced in skeletal muscle of malnourished animals [62,63]. The fact that we explored 4EBP1 and p70S6K activation in the starved state, and not challenged by insulin, could in part explain the lack of changes reported in the present study. Also, we cannot exclude that exploring these signaling pathways after 8 weeks of energy-protein restriction might be too late to observe significant changes in protein synthesis in skeletal muscles. Akt activation is known to stimulate mTORC1 to activate protein synthesis in response to insulin [61]. Here, we observed an activation of Akt in *biceps femoris* and *trapezius* in malnourished minipigs. The trends for downregulation of muscle mRNA myostatin levels we report in muscle of malnourished minipigs may play a role in Akt activation since this transforming growth factor is recognized to negatively regulate the activity of Akt [64]. Even if previous studies observed a similar activation of Akt in energy-restricted rodents [22,65], this result should have impacted mTORC1 signaling pathways, and especially 4EBP1 and p70S6K. The activation of Akt in skeletal muscle from malnourished minipigs suggest that muscle insulin sensitivity may be improved to allow a better muscle glucose uptake *via* the action of Akt on GLUT4 translocation [65]. The lack of impact of Akt on protein synthesis could be explained by the concomitant activation of AMPK, recognized as an inhibitor of muscle protein synthesis through the down-regulation of mTOR signaling, and this downstream of the action of Akt [66]. Several mechanisms also contribute to proteolysis in atrophied skeletal muscle, including the activation of calpains, caspases, ubiquitin-proteasome and autophagy-lysosome systems [7]. In the present study in malnourished minipigs, we did not observe changes of ubiquitinated proteins, nor of the ubiquitinase ligase MuRF1. As previously reported in rodent and humans in response to short- and long-term disuse atrophy [67–69], we cannot exclude that

proteolysis was mainly activated during the first days and weeks of energy-protein restriction, and that exploring these signaling pathways after 8 weeks was too late to observe this phenomenon.

Conclusion. In summary, our results support that our experimental minipig model of severe malnutrition is valid to mimic changes in body weight, body composition, gut microbiota, histological and molecular skeletal muscle patterns occurring in human protein-energy malnutrition. The blood biomarkers we measured suggest that our model is close to marasmus and severe malnutrition observed in anorexia nervosa. Our model should be useful to better understanding the pathophysiological mechanisms of muscle atrophy associated with malnutrition, as observed in patients with secondary sarcopenia, and to test new therapeutics against human marasmus malnutrition.

ACKNOWLEDGEMENTS

We thank all the staff from the Rennes pig experimental facilities (UE3P), and especially Julien George, Josselin Delamarre, Francis Le Gouevec, Alain Chauvin and Serge Dubois, for taking care of the animals and helping during the experimental period. We also thank all the staff from the NuMeCan research department who was involved in the biological sampling and treatment, and especially Armelle Cahu, Laurence Le Normand, Isabelle Nogret and Régis Janvier.

FUNDING STATEMENT

Laurence Lacaze received in the context of this project two research grants from the Société Francophone de Nutrition Clinique et Métabolisme (SFNCM) and the Association de Chirurgie Hépato-Bilio-Pancréatique et Transplantation Hépatique (ACHBT). Part of the project was also funded by INRAE.

CONFLICT OF INTEREST

No conflicts of interest, financial or otherwise, are declared by the authors.

CREDIT AUTHOR STATEMENT

Laurence Lacaze: Conceptualization, Methodology, Investigation, Writing- Original Draft, Visualization, Formal analysis, Funding acquisition. **Sarah Rochdi**: Investigation, Formal analysis. **Annaëlle Couvert**: Investigation, Formal analysis. **Steve Touboulic**: Investigation, Formal analysis. **Sylvie Guérin**: Investigation, Formal analysis. **Gwénaëlle Randuineau**: Formal analysis. **David Martin :** Investigation, Formal analysis. **Véronique Romé**: Formal analysis. **Charles-Henri Malbert**: Methodology, Investigation. **Frédéric Derbré**: Writing-Original Draft, Visualization, Formal analysis, Supervision, Funding acquisition. **David Val-Laillet**: Conceptualization, Methodology, Writing - Review & Editing, Supervision, Project administration, Funding acquisition. **Ronan Thibault**: Conceptualization, Methodology, Writing - Review & Editing, Supervision, Project administration, Funding acquisition.

REFERENCES

[1] Inotai A, Nuijten M, Roth E, Hegazi R, Kaló Z. Modelling the burden of disease associated malnutrition. E-SPEN J 2012;7:e196–204. https://doi.org/10.1016/j.clnme.2012.07.003.

[2] Snider JT, Linthicum MT, Wu Y, LaVallee C, Lakdawalla DN, Hegazi R, et al. Economic Burden of Community-Based Disease-Associated Malnutrition in the United States. J Parenter Enter Nutr 2014;38:77S-85S. https://doi.org/10.1177/0148607114550000.

[3] Barazzoni R, Gortan Cappellari G. Double burden of malnutrition in persons with obesity. Rev Endocr Metab Disord 2020;21:307–13. https://doi.org/10.1007/s11154-020-09578-1.

[4] Risi R, Tuccinardi D, Mariani S, Lubrano C, Manfrini S, Donini LM, et al. Liver disease in obesity and underweight: the two sides of the coin. A narrative review. Eat Weight Disord EWD 2021;26:2097–107. https://doi.org/10.1007/s40519-020-01060-w.

[5] Cederholm T, Barazzoni R, Austin P, Ballmer P, Biolo G, Bischoff SC, et al. ESPEN guidelines on definitions and terminology of clinical nutrition. Clin Nutr Edinb Scotl 2017;36:49–64. https://doi.org/10.1016/j.clnu.2016.09.004.

[6] Sieber CC. Malnutrition and sarcopenia. Aging Clin Exp Res 2019;31:793–8. https://doi.org/10.1007/s40520-019-01170-1.

[7] Pierre N, Appriou Z, Gratas-Delamarche A, Derbré F. From physical inactivity to immobilization: Dissecting the role of oxidative stress in skeletal muscle insulin resistance and atrophy. Free Radic Biol Med 2016;98:197–207. https://doi.org/10.1016/j.freeradbiomed.2015.12.028.

[8] Miyamoto Y, Hanna DL, Zhang W, Baba H, Lenz H-J. Molecular Pathways: Cachexia Signaling-A Targeted Approach to Cancer Treatment. Clin Cancer Res Off J Am Assoc Cancer Res 2016;22:3999–4004. https://doi.org/10.1158/1078-0432.CCR-16-0495.

[9] Brioche T, Lemoine-Morel S. Oxidative Stress, Sarcopenia, Antioxidant Strategies and Exercise: Molecular Aspects. Curr Pharm Des 2016;22:2664–78. https://doi.org/10.2174/1381612822666160219120531.

[10] Bechet D, Tassa A, Taillandier D, Combaret L, Attaix D. Lysosomal proteolysis in skeletal muscle. Int J Biochem Cell Biol 2005;37:2098–114. https://doi.org/10.1016/j.biocel.2005.02.029.

[11] Guillet C, Prod'homme M, Balage M, Gachon P, Giraudet C, Morin L, et al. Impaired anabolic response of muscle protein synthesis is associated with S6K1 dysregulation in elderly humans. FASEB J Off Publ Fed Am Soc Exp Biol 2004;18:1586–7. https://doi.org/10.1096/fj.03-1341fje.

[12] Paddon-Jones D, Sheffield-Moore M, Cree MG, Hewlings SJ, Aarsland A, Wolfe RR, et al. Atrophy and impaired muscle protein synthesis during prolonged inactivity and stress. J Clin Endocrinol Metab 2006;91:4836–41. https://doi.org/10.1210/jc.2006-0651.

[13] White JP, Baynes JW, Welle SL, Kostek MC, Matesic LE, Sato S, et al. The regulation of skeletal muscle protein turnover during the progression of cancer cachexia in the Apc(Min/+) mouse. PloS One 2011;6:e24650. https://doi.org/10.1371/journal.pone.0024650.

[14] Gundersen K, Bruusgaard JC. Nuclear domains during muscle atrophy: nuclei lost or paradigm lost? J Physiol 2008;586:2675–81. https://doi.org/10.1113/jphysiol.2008.154369.

[15] Wang H, Listrat A, Meunier B, Gueugneau M, Coudy-Gandilhon C, Combaret L, et al. Apoptosis in capillary endothelial cells in ageing skeletal muscle. Aging Cell 2014;13:254–62. https://doi.org/10.1111/acel.12169.

[16] Hanachi M, Manichanh C, Schoenenberger A, Pascal V, Levenez F, Cournède N, et al. Altered host-gut microbes symbiosis in severely malnourished anorexia nervosa (AN) patients undergoing enteral nutrition: An explicative factor of functional

intestinal disorders? Clin Nutr Edinb Scotl 2019;38:2304–10. https://doi.org/10.1016/j.clnu.2018.10.004.

[17] Masuoka H, Suda W, Tomitsuka E, Shindo C, Takayasu L, Horwood P, et al. The influences of low protein diet on the intestinal microbiota of mice. Sci Rep 2020;10:17077. https://doi.org/10.1038/s41598-020-74122-9.

[18] Smith MI, Yatsunenko T, Manary MJ, Trehan I, Mkakosya R, Cheng J, et al. Gut microbiomes of Malawian twin pairs discordant for kwashiorkor. Science 2013;339:548–54. https://doi.org/10.1126/science.1229000.

[19] Zhao J, Huang Y, Yu X. A Narrative Review of Gut-Muscle Axis and Sarcopenia: The Potential Role of Gut Microbiota. Int J Gen Med 2021;14:1263–73. https://doi.org/10.2147/IJGM.S301141.

[20] Dong J, Yu J, Li Z, Gao S, Wang H, Yang S, et al. Serum insulin-like growth factor binding protein 2 levels as biomarker for pancreatic ductal adenocarcinoma-associated malnutrition and muscle wasting. J Cachexia Sarcopenia Muscle 2021;12:704–16. https://doi.org/10.1002/jcsm.12692.

[21] Campos F, Abrigo J, Aguirre F, Garcés B, Arrese M, Karpen S, et al. Sarcopenia in a mice model of chronic liver disease: role of the ubiquitin-proteasome system and oxidative stress. Pflugers Arch 2018;470:1503–19. https://doi.org/10.1007/s00424-018-2167-3.

[22] van den Hoek AM, Zondag GCM, Verschuren L, de Ruiter C, Attema J, de Wit EC, et al. A novel nutritional supplement prevents muscle loss and accelerates muscle mass recovery in caloric-restricted mice. Metabolism 2019;97:57–67. https://doi.org/10.1016/j.metabol.2019.05.012.

[23] Hirabayashi T, Nakanishi R, Tanaka M, Nisa BU, Maeshige N, Kondo H, et al. Reduced metabolic capacity in fast and slow skeletal muscle via oxidative stress and

the energy-sensing of AMPK/SIRT1 in malnutrition. Physiol Rep 2021;9:e14763. https://doi.org/10.14814/phy2.14763.

[24] Val-Laillet D. Review: Impact of food, gut-brain signals and metabolic status on brain activity in the pig model: 10 years of nutrition research using in vivo brain imaging. Anim Int J Anim Biosci 2019;13:2699–713. https://doi.org/10.1017/S1751731119001745.

[25] Polakof S, Rémond D, David J, Dardevet D, Savary-Auzeloux I. Time-course changes in circulating branched-chain amino acid levels and metabolism in obese Yucatan minipig. Nutr Burbank Los Angel Cty Calif 2018;50:66–73. https://doi.org/10.1016/j.nut.2017.11.004.

[26] Miller ER, Ullrey DE. The pig as a model for human nutrition. Annu Rev Nutr 1987;7:361–82. https://doi.org/10.1146/annurev.nu.07.070187.002045.

[27] Val-Laillet D, Blat S, Louveau I, Malbert CH. A computed tomography scan application to evaluate adiposity in a minipig model of human obesity. Br J Nutr 2010;104:1719–28. https://doi.org/10.1017/S0007114510002667.

[28] Lemaire M, Dou S, Cahu A, Formal M, Le Normand L, Romé V, et al. Addition of dairy lipids and probiotic Lactobacillus fermentum in infant formula programs gut microbiota and entero-insular axis in adult minipigs. Sci Rep 2018;8:11656. https://doi.org/10.1038/s41598-018-29971-w.

[29] Escudié F, Auer L, Bernard M, Mariadassou M, Cauquil L, Vidal K, et al. FROGS: Find, Rapidly, OTUs with Galaxy Solution. Bioinforma Oxf Engl 2018;34:1287–94. https://doi.org/10.1093/bioinformatics/btx791.

[30] Magoč T, Salzberg SL. FLASH: fast length adjustment of short reads to improve genome assemblies. Bioinformatics 2011;27:2957–63. https://doi.org/10.1093/bioinformatics/btr507.

[31] Martin M. Cutadapt removes adapter sequences from high-throughput sequencing reads. EMBnetJournal 2011;17:10. https://doi.org/10.14806/ej.17.1.200.

[32] Mahé F, Rognes T, Quince C, de Vargas C, Dunthorn M. Swarm v2: highly-scalable and high-resolution amplicon clustering. PeerJ 2015;3:e1420. https://doi.org/10.7717/peerj.1420.

[33] Rognes T, Flouri T, Nichols B, Quince C, Mahé F. VSEARCH: a versatile open source tool for metagenomics. PeerJ 2016;4:e2584. https://doi.org/10.7717/peerj.2584.

[34] Bokulich NA, Subramanian S, Faith JJ, Gevers D, Gordon JI, Knight R, et al. Quality-filtering vastly improves diversity estimates from Illumina amplicon sequencing. Nat Methods 2013;10:57–9. https://doi.org/10.1038/nmeth.2276.

[35] Quast C, Pruesse E, Yilmaz P, Gerken J, Schweer T, Yarza P, et al. The SILVA ribosomal RNA gene database project: improved data processing and web-based tools. Nucleic Acids Res 2013;41:D590-596. https://doi.org/10.1093/nar/gks1219.

[36] Behan WMH, Cossar DW, Madden HA, McKay IC. Validation of a simple, rapid, and economical technique for distinguishing type 1 and 2 fibres in fixed and frozen skeletal muscle. J Clin Pathol 2002;55:375–80. https://doi.org/10.1136/jcp.55.5.375.

[37] Schneider CA, Rasband WS, Eliceiri KW. NIH Image to ImageJ: 25 years of image analysis. Nat Methods 2012;9:671–5.

[38] Cederholm T, Jensen GL, Correia MITD, Gonzalez MC, Fukushima R, Higashiguchi T, et al. GLIM criteria for the diagnosis of malnutrition – A consensus report from the global clinical nutrition community. Clin Nutr 2019;38:1–9. https://doi.org/10.1016/j.clnu.2018.08.002.

[39] Polito A, Cuzzolaro M, Raguzzini A, Censi L, Ferro-Luzzi A. Body composition changes in anorexia nervosa. Eur J Clin Nutr 1998;52:655–62. https://doi.org/10.1038/sj.ejcn.1600618.

[40] McLoughlin DM, Spargo E, Wassif WS, Newham DJ, Peters TJ, Lantos PL, et al. Structural and functional changes in skeletal muscle in anorexia nervosa. Acta Neuropathol (Berl) 1998;95:632–40. https://doi.org/10.1007/s004010050850.

[41] Petersen JS, Henckel P, Oksbjerg N, Sørensen MT. Adaptations in muscle fibre characteristics induced by physical activity in pigs. Anim Sci 1998;66:733–40. https://doi.org/10.1017/S1357729800009310.

[42] Lindboe CF, Askevold F, Slettebø M. Changes in skeletal muscles of young women with anorexia nervosa. An enzyme histochemical study. Acta Neuropathol (Berl) 1982;56:299–302. https://doi.org/10.1007/BF00691262.

[43] Lewis MI, Sieck GC, Fournier M, Belman MJ. Effect of nutritional deprivation on diaphragm contractility and muscle fiber size. J Appl Physiol Bethesda Md 1985 1986;60:596–603. https://doi.org/10.1152/jappl.1986.60.2.596.

[44] Slettebø M, Lindboe CF, Askevold F. The neuromuscular system in patients with anorexia nervosa: electrophysiological and histologic studies. Clin Neuropathol 1984;3:217–24.

[45] Madeira MS, Pires VMR, Alfaia CM, Lopes PA, Martins SV, Pinto RMA, et al. Restriction of dietary protein does not promote hepatic lipogenesis in lean or fatty pigs. Br J Nutr 2016;115:1339–51. https://doi.org/10.1017/S0007114516000453.

[46] Srikantia SG, Jacob CM, Reddy V, Hyderabad T. SERUM ENZYME LEVELS IN PROTEIN-CALORIE MALNUTRITION. STUDIES IN CHILDREN WITH KWASHIORKOR AND MARASMUS. Am J Dis Child 1960 1964;107:256–9. https://doi.org/10.1001/archpedi.1964.02080060258006.

[47] Taiwo OO, Thomas KD. Plasma biochemical parameters in Nigerian children with protein energy malnutrition. East Afr Med J 1992;69:428–32.

[48] Mira M, Stewart PM, Vizzard J, Abraham S. Biochemical abnormalities in anorexia nervosa and bulimia. Ann Clin Biochem 1987;24 (Pt 1):29–35. https://doi.org/10.1177/000456328702400104.

[49] El-Hodhod MA, Emam EK, Zeitoun YA, El-Araby AM. Serum ghrelin in infants with protein-energy malnutrition. Clin Nutr Edinb Scotl 2009;28:173–7. https://doi.org/10.1016/j.clnu.2009.02.003.

[50] Hari P, Bagga A, Mahajan P, Lakshmy R. Effect of malnutrition on serum creatinine and cystatin C levels. Pediatr Nephrol Berl Ger 2007;22:1757–61. https://doi.org/10.1007/s00467-007-0535-x.

[51] Bilancio G, Lombardi C, Pisot R, De Santo NG, Cavallo P, Cirillo M. Effects of bed-rest on urea and creatinine: correlation with changes in fat-free mass. PloS One 2014;9:e108805. https://doi.org/10.1371/journal.pone.0108805.

[52] Kameda M, Teruya T, Yanagida M, Kondoh H. Reduced uremic metabolites are prominent feature of sarcopenia, distinct from antioxidative markers for frailty. Aging 2021;13:20915–34. https://doi.org/10.18632/aging.203498.

[53] Paniagua R, Santos D, Muñoz R, Luengas J, Frenk S. Renal function in protein-energy malnutrition. Pediatr Res 1980;14:1260–2. https://doi.org/10.1203/00006450-198011000-00021.

[54] Riva A, Pigni M, Nacinovich R. Renal dysfunctions and clinical correlates in adolescents with restrictive anorexia nervosa. Clin Nutr ESPEN 2021;43:230–4. https://doi.org/10.1016/j.clnesp.2021.04.011.

[55] Wada Y, Komatsu Y, Izumi H, Shimizu T, Takeda Y, Kuwahata M. Increased Ratio of Non-mercaptalbumin-1 Among Total Plasma Albumin Demonstrates Potential Protein Undernutrition in Adult Rats. Front Nutr 2018;5:64. https://doi.org/10.3389/fnut.2018.00064.

[56] Hubert MF, Laroque P, Gillet JP, Keenan KP. The effects of diet, ad Libitum feeding, and moderate and severe dietary restriction on body weight, survival, clinical pathology parameters, and cause of death in control Sprague-Dawley rats. Toxicol Sci Off J Soc Toxicol 2000;58:195–207. https://doi.org/10.1093/toxsci/58.1.195.

[57] Blanton LV, Charbonneau MR, Salih T, Barratt MJ, Venkatesh S, Ilkaveya O, et al. Gut bacteria that prevent growth impairments transmitted by microbiota from malnourished children. Science 2016;351:aad3311. https://doi.org/10.1126/science.aad3311.

[58] Morita C, Tsuji H, Hata T, Gondo M, Takakura S, Kawai K, et al. Gut Dysbiosis in Patients with Anorexia Nervosa. PLoS ONE 2015;10:e0145274. https://doi.org/10.1371/journal.pone.0145274.

[59] Kleiman SC, Watson HJ, Bulik-Sullivan EC, Huh EY, Tarantino LM, Bulik CM, et al. The Intestinal Microbiota in Acute Anorexia Nervosa and During Renourishment: Relationship to Depression, Anxiety, and Eating Disorder Psychopathology. Psychosom Med 2015;77:969–81. https://doi.org/10.1097/PSY.0000000000000247.

[60] Jäger S, Handschin C, St-Pierre J, Spiegelman BM. AMP-activated protein kinase (AMPK) action in skeletal muscle via direct phosphorylation of PGC-1alpha. Proc Natl Acad Sci U S A 2007;104:12017–22. https://doi.org/10.1073/pnas.0705070104.

[61] Yoon M-S. mTOR as a Key Regulator in Maintaining Skeletal Muscle Mass. Front Physiol 2017;8:788. https://doi.org/10.3389/fphys.2017.00788.

[62] Wykes LJ, Fiorotto M, Burrin DG, Del Rosario M, Frazer ME, Pond WG, et al. Chronic low protein intake reduces tissue protein synthesis in a pig model of protein malnutrition. J Nutr 1996;126:1481–8. https://doi.org/10.1093/jn/126.5.1481.

[63] Salles J, Chanet A, Berry A, Giraudet C, Patrac V, Domingues-Faria C, et al. Fast digestive, leucine-rich, soluble milk proteins improve muscle protein anabolism, and

mitochondrial function in undernourished old rats. Mol Nutr Food Res 2017;61. https://doi.org/10.1002/mnfr.201700287.

[64] Rodriguez J, Vernus B, Chelh I, Cassar-Malek I, Gabillard JC, Hadj Sassi A, et al. Myostatin and the skeletal muscle atrophy and hypertrophy signaling pathways. Cell Mol Life Sci CMLS 2014;71:4361–71. https://doi.org/10.1007/s00018-014-1689-x.

[65] Gavete ML, Martín MA, Alvarez C, Escrivá F. Maternal food restriction enhances insulin-induced GLUT-4 translocation and insulin signaling pathway in skeletal muscle from suckling rats. Endocrinology 2005;146:3368–78. https://doi.org/10.1210/en.2004-1658.

[66] Bolster DR, Crozier SJ, Kimball SR, Jefferson LS. AMP-activated protein kinase suppresses protein synthesis in rat skeletal muscle through down-regulated mammalian target of rapamycin (mTOR) signaling. J Biol Chem 2002;277:23977–80. https://doi.org/10.1074/jbc.C200171200.

[67] Chopard A, Lecunff M, Danger R, Lamirault G, Bihouee A, Teusan R, et al. Large-scale mRNA analysis of female skeletal muscles during 60 days of bed rest with and without exercise or dietary protein supplementation as countermeasures. Physiol Genomics 2009;38:291–302. https://doi.org/10.1152/physiolgenomics.00036.2009.

[68] Salaun E, Lefeuvre-Orfila L, Cavey T, Martin B, Turlin B, Ropert M, et al. Myriocin prevents muscle ceramide accumulation but not muscle fiber atrophy during short-term mechanical unloading. J Appl Physiol Bethesda Md 1985 2016;120:178–87. https://doi.org/10.1152/japplphysiol.00720.2015.

[69] Derbre F, Ferrando B, Gomez-Cabrera MC, Sanchis-Gomar F, Martinez-Bello VE, Olaso-Gonzalez G, et al. Inhibition of xanthine oxidase by allopurinol prevents skeletal muscle atrophy: role of p38 MAPKinase and E3 ubiquitin ligases. PloS One 2012;7:e46668. https://doi.org/10.1371/journal.pone.0046668.

Table 1. Composition and nutritional values of the two isocaloric diets given to the Yucatan minipigs for 8 weeks: the standard diet (ST) or the low-calorie/low-protein (LC/LP) diet.

	Standard diet	**LC/LP diet**
Soft wheat (%)	10	30.77
Barley (%)	33	10
Soft wheat bran (%)	25	25
Soybean hulls (%)	12	12
Dry beet pulp (%)	/	5
Soybean meal 48 (%)	6	/
Unshelled sunflower meal (%)	10	/
Molasses (%)	1	1
Corn starch	/	8.14
Sugar	/	/
Cellulose	/	5
Sodium chlorure	0.6	0.6
Calcium carbonate	1.3	1.1
Dicalcium phosphate	0.6	0.89
Mineral vitaminic complement	0.5	0.5
Total	100	100
EM (MJ/kg)	10.33	10.37
EM (kcal/kg)	2470	2479
MAD/EN	15	8.63

EM, metabolisable energy; EN: net energy; MAD: digestible nitrogenous matter.

Table 2. Biological plasma analyses in Yucatan minipigs subjected to a standard diet (ST) or low-calorie/low-protein (LC/LP) for 8 weeks. Values are expressed as mean ± SD. Significance was checked using Mann-Whitney test. Significant differences are indicated in bold/italic. *ALT, alanine aminotransferase; AST, aspartate aminotransferase; CRP, C-reactive protein.*

VARIABLES	ST group	LC/LP group	*P-value*
Urea (mg/dl)	33.86±8.82	23.52±4.07	***0.008***
Creatinine (mg/dl)	1.55±0.09	1.81±0.15	***0.017***
Glucose (g/l)	0.65±0.15	0.74±0.08	0.34
Albumin (g/l)	46.39±3.2	44.72±5.7	0.77
AST (IU/l)	79.34±19.7	41.04±11.9	***0.02***
ALT (IU/l)	55.2±13	38.97±7.4	***0.05***
CRP (µg/ml)	38.2±26.8	32.8±24.6	0.79

FIGURE LEGENDS

Figure 1. Body weight and body composition assessed by computed tomography (CT-scan) in minipigs subjected to a standard diet (ST) or low-calorie/low-protein (LC/LP) for 8 weeks. ~~*B*~~*A*: Evolution of body weight. ~~in ST and LC/LP animals~~ ~~*BC-F:*~~ Evolution of muscle T13 area. ~~in ST and LC/LP animals~~ *C:* Evolution of visceral fat mass area. ~~*GD:*~~ Representative picture of CT-scan slices with in red, either the threshold for muscle (from -29 to +150 HU) or fat (from -190 to -30 HU). The yellow delineations include *Longissimus dorsi, Psoas major and large muscle,* as well as abdominal muscles on the left panel, and the retroperitoneal fat tissue on the right panel. Values are shown as paired individual mean values (n=5-6/group). Significance was checked using Wilcoxon test. Significant differences between T0 and T8: **P*<0.05.

Figure 2. Muscle fiber size in minipigs subjected to a standard diet (ST) or low-calorie/low-protein (LC/LP) for 8 weeks. *A-C*: Muscle fiber cross-sectional area (CSA) histological analyses and frequency distribution of muscle CSA in the *trapezius* after 8 weeks of standard (n=5) or LC/LP (n=6) diets. *D-F*: Muscle fiber cross-sectional area (CSA) histological analyses in the *biceps femoris* after 8 weeks of standard (n=5) or LC/LP diet (n=6). G: Representative immunohistochemistry images for type 1 slow (dark) and type 2 fast (blank) fibers from *trapezius*. H-I: cross-sectional area (CSA) of type 1 slow and type 2 fast fibers in the *trapezius* after 8 weeks of standard (n=5) or LC/LP diet (n=6).

Values are expressed as mean ± SD. Significance was checked using Mann-Whitney test. Significant differences between ST and LC/LP groups: *** *P*<0.001.

Figure 3. Gut microbiota composition of minipigs subjected to a standard diet (ST) or low-calorie/low-protein (LC/LP) for 8 weeks. *A-B:* Richness and α-diversity indexes before and after 8 weeks of ST (A) or LC/LP (B) diets. *C:* Abundance of the main phyla before and after 8 weeks of ST or LC/LP diets. *D:* Principal component analysis (PCA) diagram using Bray–Curtis distances on the normalized abundance of OTUs before and after 8 weeks of ST (D) or LC/LP diets (E). *F:* Relationship between the variations of number of observed species and body weight before and after 8 weeks of ST or LC/LP diets. Significant differences before and after 8 weeks of LC/LP diet: * $P<0.05$, Wilcoxon test.

Figure 4. Energy metabolism and atrophy signalling pathways in skeletal muscle of minipigs subjected to a standard diet (ST) or low-calorie/low-protein (LC/LP) for 8 weeks. Representative images of Western Blot performed in *trapezius* (A) and *biceps femoris* (C). Total content or phosphorylation of signalling proteins involved in energy metabolism and atrophy in *trapezius* (B) and *biceps femoris* (D). Data are presented as fold change in LC/LP compared to ST group (mean ± SD, n=5-6). Significance was checked using Mann-Whitney test. Significant differences between ST and LC/LP groups: * $P<0.05$; ** $P<0.01$.

Figure 5. Expression of genes coding for myostatin, MuRF1 and MAFbx in the *trapezius* (A) and *biceps femoris* (B) muscles in minipigs subjected to a standard diet (ST) or low-calorie/low-protein (LC/LP) for 8 weeks. Data are presented as fold change in LC/LP compared to ST group (mean ± SD, n=5-6). Significance was checked using Mann-Whitney test.

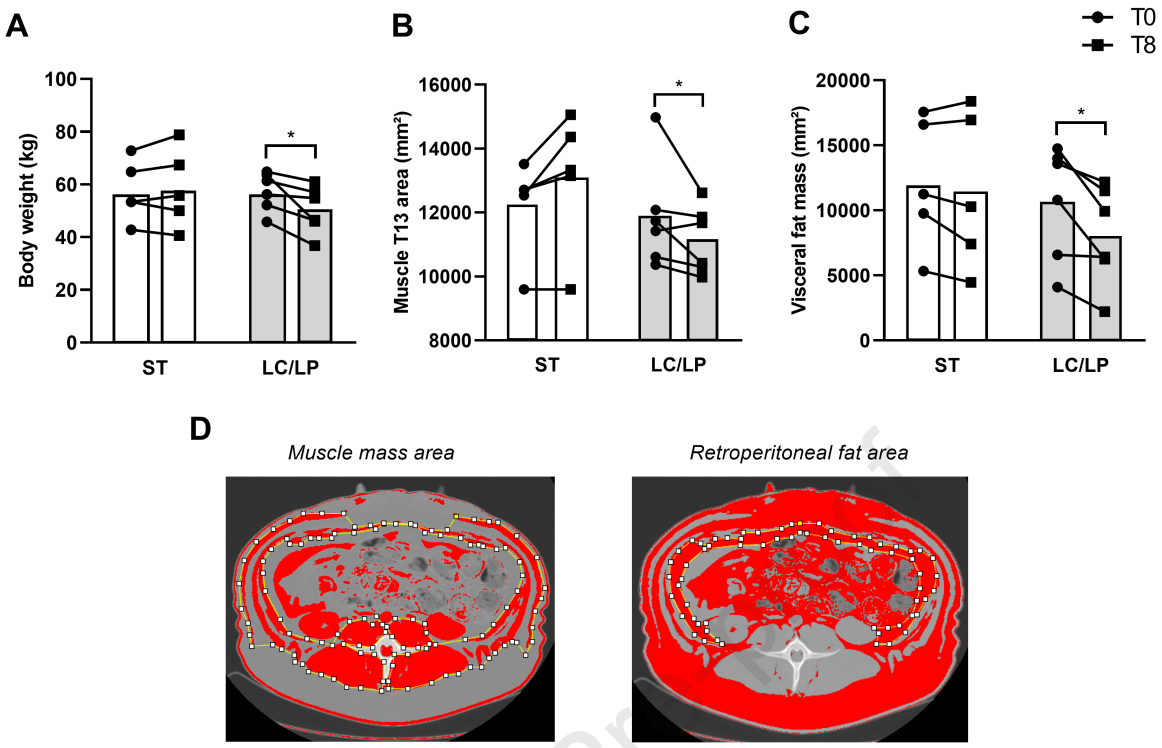

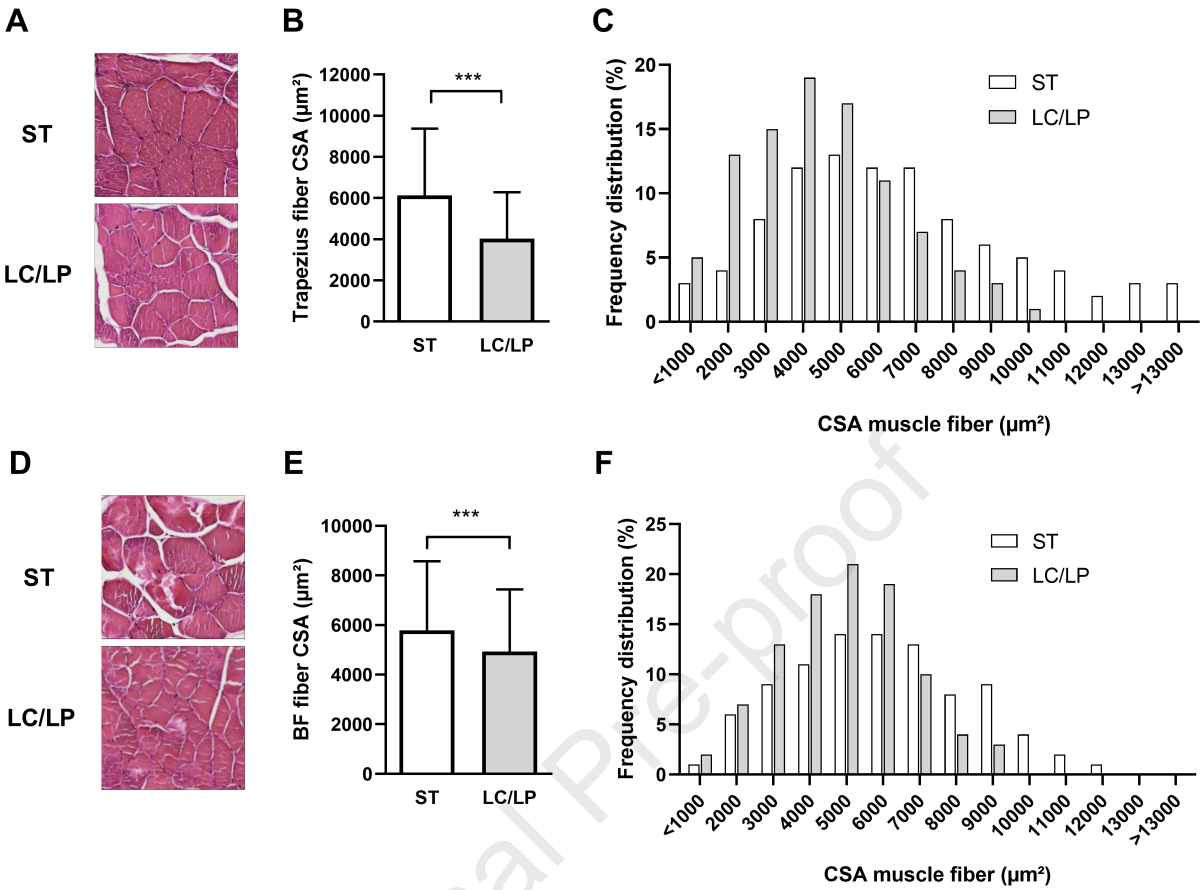

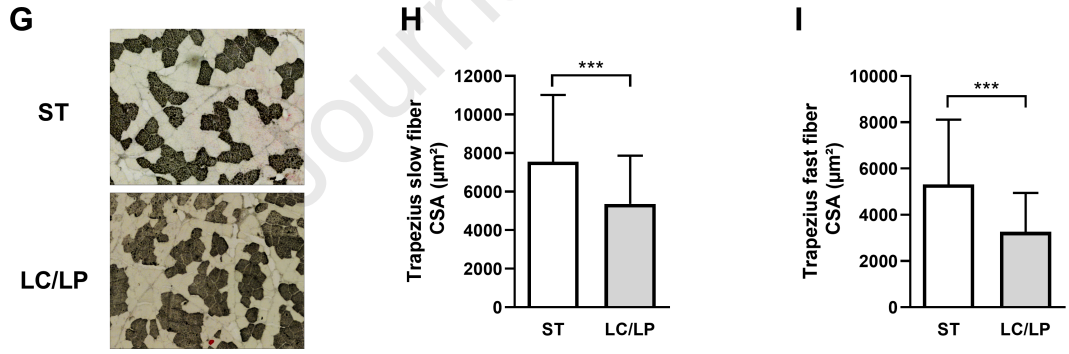

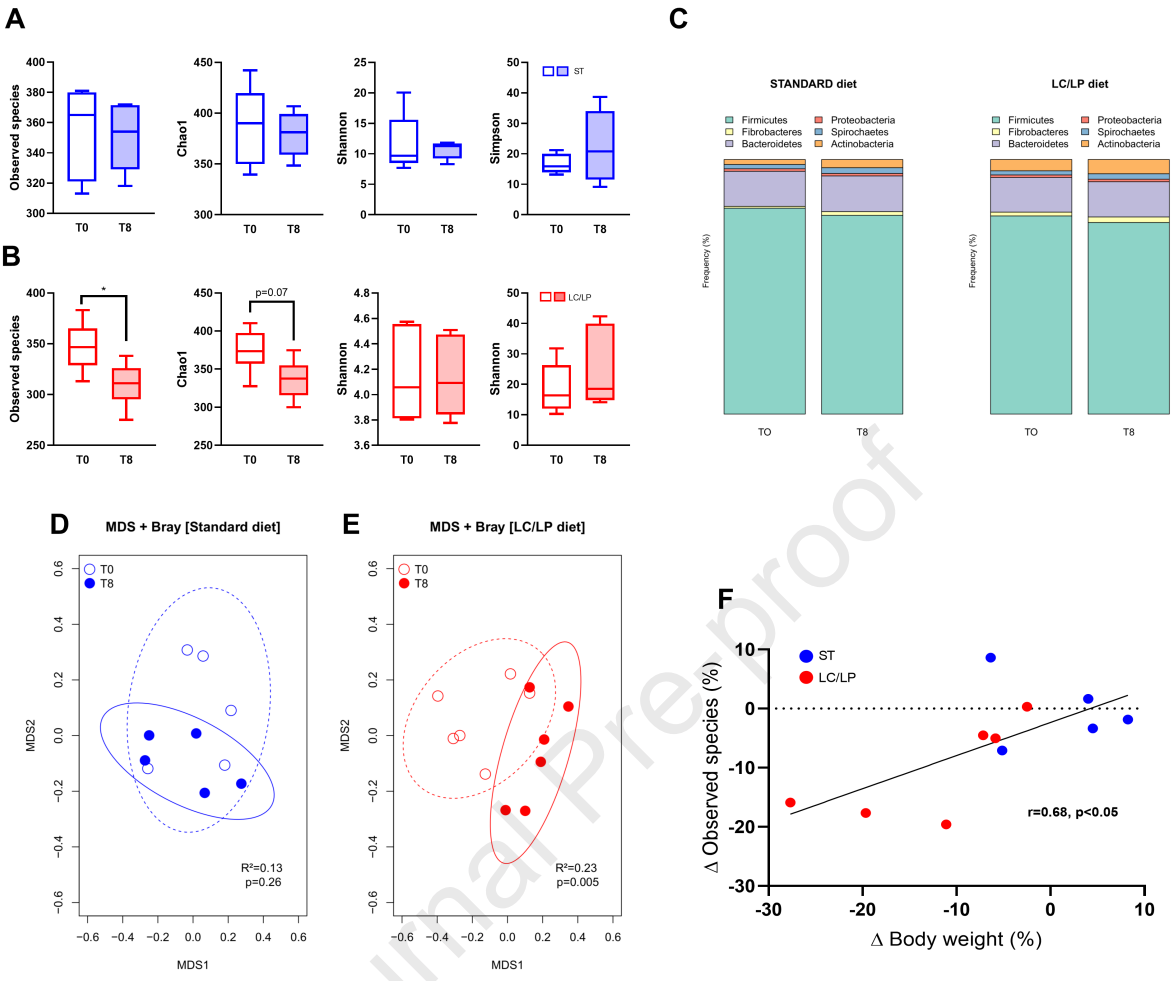

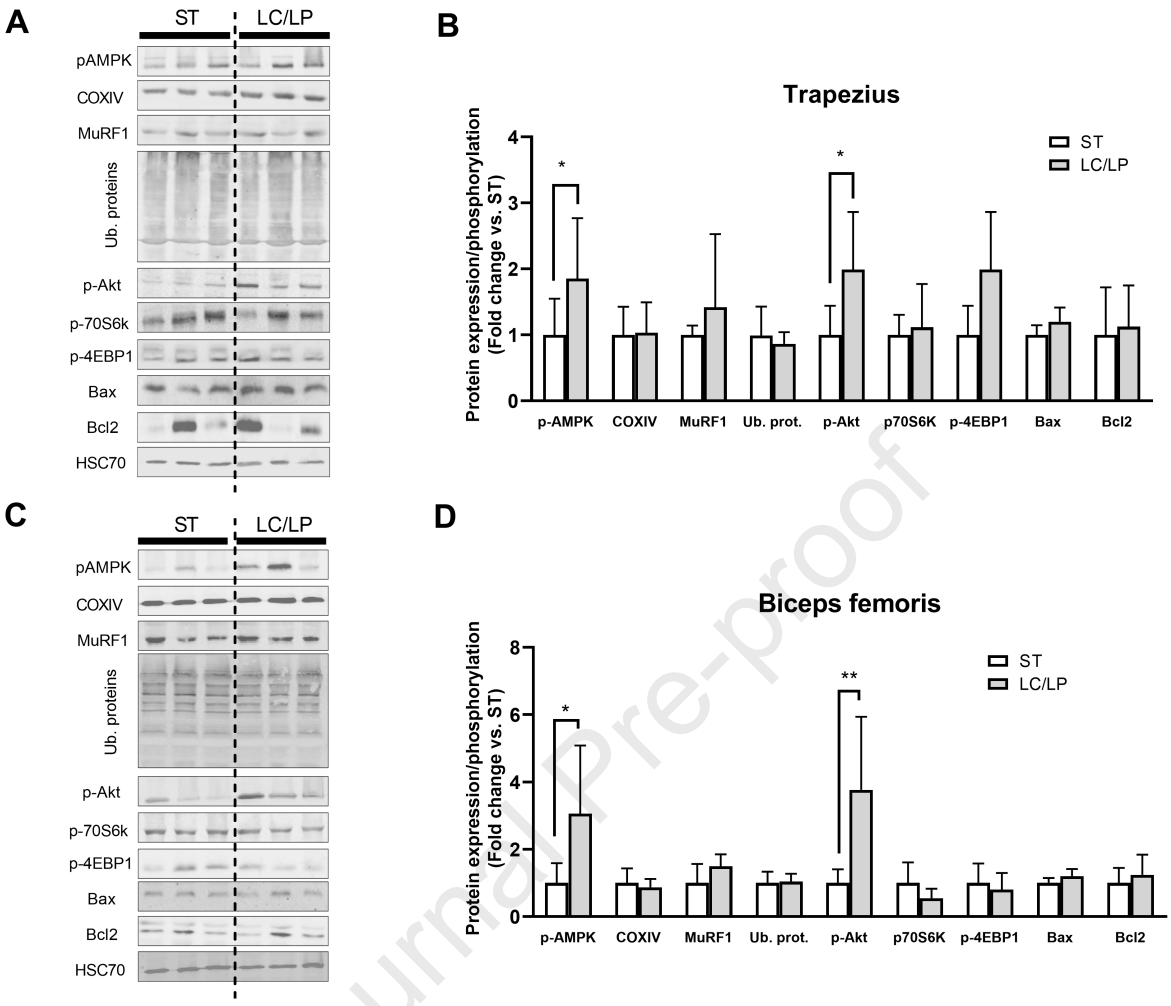

A

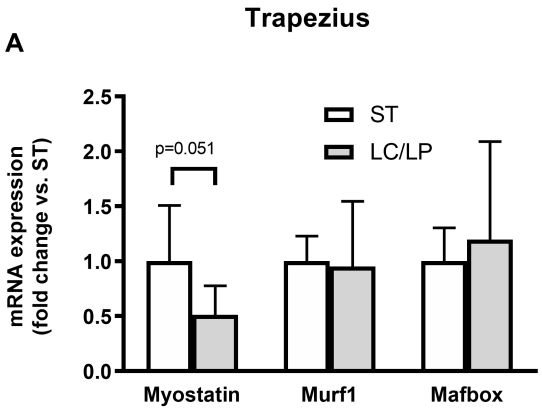

B